

# Evaporation of the accretion disk in dwarf novae during quiescence

B.F. Liu<sup>1,2</sup>, F. Meyer<sup>1</sup>, and E. Meyer-Hofmeister<sup>1</sup>

<sup>1</sup> Max-Planck-Institut für Astrophysik, Karl-Schwarzschild-Str.1, D-85740 Garching, Germany

<sup>2</sup> Yunnan Observatory, Academia Sinica, P.O. Box 110, Kunming 650011, China

Received 22 April 1997 / Accepted 4 July 1997

**Abstract.** We investigate the evolution of the accretion disk in dwarf nova systems during quiescence. This is the phase of accumulation of matter in the disk. We employ the evaporation model of Meyer & Meyer-Hofmeister (1994) in which above the cool inert disk, a self-sustained coronal layer is built up, fed by matter evaporating from the disk underneath. Conservation of mass and angular momentum governs the evolution of the coexisting cool disk and corona. We compute the evolution and show how the onset of the next outburst is influenced by the evaporation process.

**Key words:** accretion, accretion disk – cataclysmic variables – stars: white dwarfs – stars: coronae

---

## 1. Introduction

Dwarf novae show alternating phases of low and high luminosity. In these binaries mass flows over from a Roche Lobe filling main sequence star via an accretion disk onto the white dwarf. During quiescence mass is accumulated in the disk until the next outburst is triggered and the material starts flowing at a rate of about  $10^{-9} M_{\odot}/\text{yr}$  towards the compact object, leading to a significant increase of luminosity.

The mass flow rate through the cool disk during quiescence is only  $10^{-12} M_{\odot}/\text{yr}$  to  $10^{-13} M_{\odot}/\text{yr}$  in the standard model for dwarf nova outbursts. But it could be shown that a self-sustained hot corona exists above this cool inert disk (Meyer & Meyer-Hofmeister 1994, Liu et al. 1995). This corona supports an accretion mass flow of about  $10^{-11} M_{\odot}/\text{yr}$  and is fed from the cool underlying disk. This leads to an evaporation of the inner disk during quiescence.

The aim of this work is to study the structural evolution of the accretion disk around a  $1M_{\odot}$  white dwarf including this effect. We evaluate the decrease of surface density starting with the distribution of mass left over from the preceding outburst. The changes of the surface density are computed according to the mass flow rates determined by Liu et al. (1995).

The depletion of matter and formation of a hole in the disk around the white dwarf has important consequences for the next

outburst. The inner evaporated part of the disk has to be filled in on the diffusion timescale before it can display the hot UV temperatures during the early outburst (Meyer & Meyer-Hofmeister 1989). This provides a natural explanation for the delay between optical and UV radiation at rise to outburst as observed for several systems (la Dous 1994, Verbunt 1987).

## 2. The formation of a hole in the inner disk region

A number of other processes besides disk evaporation might also lead to hole formation. The desirability of hole formation had already been pointed out in Meyer & Meyer-Hofmeister (1989) where it was suggested that remaining disk magnetic field might lead to a lowering of the surface density in the inner disk region below the lower critical value for the existence of bistable disk structure. This would prevent a heating wave coming from the outside to transform the inner disk to a hot UV radiating state and is equivalent to hole formation. Later Livio & Pringle (1992) discussed as alternative to the evaporation mechanism the possibility that white dwarf magnetic fields, too weak to be observable, in other ways might sweep the interior disk matter away in quiescence. Speculative reasoning on the dwarf nova oscillation phenomenon (Meyer 1997) lets us appear the assumption of such field less attractive though does not exclude it. Another possibility to deplete an inner disk region in quiescence is to irradiate the disk surface from the still hot white dwarf and thereby raise the disk temperature which would result in mass flow towards the white dwarf (King 1997). We point out that the coronal evaporation process itself deposits heat into the underlying cool disk, possibly more important than irradiation from the white dwarf which also accelerates mass depletion during the early phase of hole formation. All such models still require coronal temperatures near the white dwarf and presumably a thermal boundary layer as discussed in Liu et al. (1995) in order to account for the observed X-rays in quiescence.

We use the evaporation model in its simple form here because it allows clear qualitative predictions in reasonable agreements with observation (Meyer & Meyer-Hofmeister 1994).

### 3. Physics of the interacting disk and corona

The evolution of the accretion disk is governed by diffusion. Conservation of mass and angular momentum give the relation between changes of surface density and mass flow in the disk. We consider here a disk which consists of a cool standard dwarf nova accretion disk near the midplane and a hot coronal disk above. The cool disk is geometrically thin, has low viscosity and a low mass flow rate. The self-sustained coronal disk is extended in vertical height, also there friction provides the energy. The mass flow rate is high, so that the situation might rather be described by a coronal flow towards the white dwarf. Close to the white dwarf the cool disk can be completely evaporated and only the hot corona exists.

In the coronal layers additional features appear. The gas pressure that supports the gas has a non-negligible radial gradient which contributes to the radial support against gravity. This lowers the demand on the centrifugal force and leads to sub-Keplerian rotation speeds, even varying with height above the midplane. The more complex rotation pattern affects the release of energy and the transport of angular momentum in these coronal layers. The deviations from the standard thin disk approximation may be measured by terms of order  $(H/r)^2$ . For a standard case ( $M=1M_{\odot}, r=10^{9.5}$  cm) this quantity is about 1/4. For a first investigation of the radial structure of an interacting cool disk and a hot corona we here neglect these effects. The viscous relaxation time in the extended corona is much shorter than that in the cool disk. The ratio of the two timescales is of the order of the ratio of the disk thickness to that of the corona squared,  $\leq 1/100$ . Thus the corona will follow the cool disk evolution in a quasi-stationary way.

The changes in the cool and in the hot coronal disk can be described as following from the conservation of mass and angular momentum in these disk layers together.  $\Sigma_d, f_d, \dot{M}_d$  are surface density, viscosity integral, and the mass flow rate of the cool disk. The corresponding values in the corona are  $\Sigma_c, f_c, \dot{M}_c$ .

The surface density and viscosity integral are defined as

$$\Sigma = \int \rho dz \quad (1)$$

and

$$f = \int \mu dz \quad (2)$$

with density  $\rho$  and vertical height  $z$ . The effective viscosity  $\mu$  is parameterized in the standard way as  $\mu = \frac{\sqrt{2}}{3} \alpha c_s \rho H_p$ ,  $\alpha$  viscosity parameter,  $c_s$  sound velocity,  $H_p$  pressure scale height. The integral extends over the cool disk ( $\Sigma_d, f_d$ ) or the corona ( $\Sigma_c, f_c$ ), both sides of the midplane together.

#### 3.1. The cool disk

The evolution of the cool disk is governed by conservation of mass and angular momentum,

$$\frac{\partial}{\partial t} (2\pi r \Sigma_d) + \frac{\partial \dot{M}_d}{\partial r} = -2\pi r \dot{m}_{d \rightarrow c} \quad (3)$$

$$\frac{\partial}{\partial t} (2\pi r \Sigma_d r^2 \Omega) + \frac{\partial}{\partial r} [(\dot{M}_d + 3\pi f_d) r^2 \Omega] = -2\pi r \dot{m}_{d \rightarrow c} r^2 \Omega \quad (4)$$

where  $\dot{m}_{d \rightarrow c}$  is the rate of mass evaporating per unit surface from disk to corona.

This gives

$$\dot{M}_d = -3\pi (f_d + 2r \frac{\partial f_d}{\partial r}) \quad (5)$$

$$\frac{\partial \Sigma_d}{\partial t} = \frac{3}{r} \frac{\partial}{\partial r} [r^{\frac{1}{2}} \frac{\partial}{\partial r} (r^{\frac{1}{2}} f_d)] - \dot{m}_{d \rightarrow c} \quad (6)$$

The typical diffusion Eq. (6) now includes the evaporation of the disk to the corona, where the evaporation term  $\dot{m}_{d \rightarrow c}$  is known from the structure of the corona. If the boundary conditions and the initial distribution of surface density are given, one can evaluate the evolution of the disk with evaporation numerically. Here we change this equation into another form which is used in our numerical computation later:

$$\frac{\partial \Sigma_d}{\partial t} = \frac{24}{x^3} \frac{\partial^2 b}{\partial x^2} - \dot{m}_{d \rightarrow c} \quad (7)$$

where  $x = 2\sqrt{r}, b = \sqrt{r} f_d$

#### 3.2. The corona above the cool disk

Here the corresponding equations are

$$\frac{\partial}{\partial t} (2\pi r \Sigma_c) + \frac{\partial \dot{M}_c}{\partial r} = 2\pi r (\dot{m}_{d \rightarrow c} - \dot{m}_w)$$

$$\frac{\partial}{\partial t} (2\pi r \Sigma_c r^2 \Omega) + \frac{\partial}{\partial r} [(\dot{M}_c + 3\pi f_c) r^2 \Omega] = 2\pi r (\dot{m}_{d \rightarrow c} - \dot{m}_w) r^2 \Omega$$

where  $\dot{m}_w$  is the rate of mass taken away by wind and we assume advective wind loss of angular momentum.

We assume that the corona is always at thermal equilibrium and is quasi-stationary. The above two equations lead to

$$\dot{M}_c = -3\pi (f_c + 2r \frac{\partial f_c}{\partial r}) \quad (8)$$

$$\dot{m}_{d \rightarrow c} = \frac{1}{2\pi r} \frac{\partial \dot{M}_c}{\partial r} + \dot{m}_w \quad (9)$$

Meyer & Meyer-Hofmeister (1994) and Liu et al. (1995) have investigated the coronal evaporation in detail and derived a scaling law for  $\dot{m}_{d \rightarrow c}$  and  $\dot{M}_{acc}$  from their numerical results. One should note that we assume that the evaporating matter takes all of its local angular momentum from the disk to the corona. From the conservation of angular momentum in both the cool disk and the hot corona it follows that part of the evaporated matter has to condense into the disk at some larger radius. In our computation, we find that the evaporation rate changes from positive to negative with radius although the absolute value of the negative amount is very small. This means that the evaporated matter partially returns to the disk. With these interactions of disk and corona, we have to generalize the results of Liu et

al. (1995) derived for a one-zone model. We take their results for the accretion rate onto the white dwarf  $\dot{M}_{acc}$  at our inner edge of the disk  $r = r_i$  and deduce from this

$$f_c(r_i) = Ar_i^{-1.2} \left(1 - \sqrt{\frac{r_{wd}}{r_i}}\right) \quad (10)$$

with  $A = 2.17 \times 10^{25} \text{ g sec cm}^{\frac{1}{2}}$ ,  $r_{wd}$  radius of the white dwarf.

With this form of  $f_c$  at the boundary, we construct a function of friction for the corona above a cool disk:

$$f_c(r, r_i) = \frac{A}{[r_i^2 + (r - r_i)^2]^{\frac{1.2}{2}}} \left(1 - \sqrt{\frac{r_{wd}}{r}}\right), r \geq r_i \quad (11)$$

The new function of friction in the corona is, of course, consistent with the coronal evaporation model (Meyer & Meyer-Hofmeister 1994, Liu et al. 1995), it has the general form  $f_c(r) \rightarrow \frac{A}{r^{1.2}}$  for  $r \gg r_i$  and fulfills  $\dot{M}_c(r_i) = \frac{-3\pi A}{r_i^{1.2}}$  as specified by the one-zone model (Meyer & Meyer-Hofmeister 1994, Liu et al. 1995). Moreover, the angular momentum flow rate derived from the new frictional function  $f_c(r, r_i)$  at the boundary is  $\sqrt{GM r_{wd}} \dot{M}_c(r_i)$ , which is just the quasi-stationary approximation for coronal gas flow.

As to the mass loss by wind, the one-zone model simplifies the innermost disk as a homogeneous area with respect to radius and determines a wind loss fraction  $\lambda = \frac{\pi r^2 \dot{m}_w}{\dot{M}_{total}}$ , i.e.  $2\pi r \dot{m}_w = \frac{2\lambda}{1-\lambda} \frac{\dot{M}_c}{r}$ . For the generalized formula we require the same scaling with radius which leads us to the following expression:

$$2\pi r \dot{m}_w = C \frac{2\lambda}{1-\lambda} \frac{3\pi f_c(r, r_i)}{[r_i^2 + (r - r_i)^2]^{\frac{1}{2}}} \quad (12)$$

The constant  $C$  normalizes the formula such that it yields the same total wind loss as the numerical value in the homogeneous one-zone model,  $\dot{M}_w = \int_{r_i}^{\infty} 2\pi r \dot{m}_w dr = \frac{\lambda}{1-\lambda} \dot{M}_c$ . This yields  $C = 0.3459$ .

With the frictional function (11) and wind mass loss expression (12), one obtains the mass evaporation rate from the cool disk to the corona above from Eqs. (8) and (9).

### 3.3. Boundary conditions

We define the radius  $r_i$  as inner boundary of the disk where the surface density decreases to zero. With the conservation of mass and angular momentum, we deduce that both the friction and mass flow rate in the disk boundary are zero, i.e.  $f_d(r_i) = 0$ ,  $(\frac{\partial f_d}{\partial r})_{r_i} = 0$ , or  $b(x_i) = 0$ ,  $(\frac{\partial b}{\partial x})_{x_i} = 0$ . This means no mass is accreted directly from the disk onto the central white dwarf. The mass in the disk is first evaporated into the corona and then flows towards the central object.

It has been known from Meyer & Meyer-Hofmeister (1994) and Liu et al. (1995) that the evaporation is much more efficient close to the white dwarf than at large distances. This implies that the first inner disk region will be evaporated and a hole is created near the white dwarf. Due to the high efficiency of

evaporation near the white dwarf such a hole grows rapidly in the innermost region of the disk. Then the inner boundary of the disk moves outwards more and more gradually. Finally it hardly moves or stalls at some radial distance until mass flowing from secondary and accumulating in the disk has reached the critical surface density and causes the onset of the next outburst.

To follow the motion of the inner boundary by evaporation, we must know the profile of  $\Sigma$  near the inner boundary. From the diffusion Eq. (7), we find an analytical approximation for the surface density there. Near the inner boundary  $x_i$ ,  $x - x_i \ll x$ , the values of  $\Sigma$  and  $b$  fall to very small values, thus the relation  $b = Bx^\nu \Sigma$  for the optically thin disk (Ludwig et al. 1994) holds, and we obtain the diffusion equation for  $b$  as

$$\frac{\partial b}{\partial t} = Bx^\nu \left( \frac{24}{x^3} \frac{\partial^2 b}{\partial x^2} - \dot{m}_{d \rightarrow c} \right) \quad (13)$$

To solve the above equation we proceed in the following way. The profile moves with a velocity  $v_i = \frac{dx_i}{dt}$  and only gradually changes its shape. For a small time step we neglect this change of shape. Then the change with time comes from the motion of the profile,  $\frac{\partial}{\partial t} = -v_i \frac{\partial}{\partial x'}$ , where  $x' = x - x_i$  is the new coordinate in the co-moving frame. To get an analytical solution for a narrow region near the inner boundary, we neglect the variation of  $Bx^\nu \frac{24}{x^3}$  and  $Bx^\nu \dot{m}_{d \rightarrow c}$  with  $x$  and regard these values as constant. Then the differential Eq. (13) becomes

$$c_2 \frac{\partial^2 b}{\partial x'^2} + c_1 \frac{\partial b}{\partial x'} + c_0 = 0 \quad (14)$$

where  $c_0 = -\dot{m}_{d \rightarrow c}$ ,  $c_1 = \frac{v_i}{Bx^\nu}$ ,  $c_2 = \frac{24}{x^3}$ .

With the boundary condition  $b = 0$  and  $\frac{\partial b}{\partial x'} = 0$  at  $x' = 0$  the solution is

$$b(x, x_i) = -\frac{c_0 c_2}{c_1^2} \left[ e^{-\frac{c_1}{c_2}(x-x_i)} - 1 + \frac{c_1}{c_2}(x-x_i) \right] \quad (15)$$

The above expression is the analytical ‘‘tail’’ of the evaporating disk near the inner boundary. The given value of  $b$  at the grid point closest to  $x_i$  determines  $c_1$ , i.e. the velocity  $v_i$  and hence the motion of the inner boundary.

## 4. Computational results of disk evolution

For a typical dwarf nova system we take the mass of the central white dwarf as  $M = 1M_\odot$ , the initial inner boundary after an outburst at  $r = 10^9 \text{ cm}$ , the outer boundary at  $3.7 \times 10^{10} \text{ cm}$ . The viscous coefficient for the cold state is taken as  $\alpha = 0.05$ .

We start our computation with the surface density distribution left over from the preceding outburst. The diffusion Eq. (7) is integrated in similar way as in earlier work (compare e.g. Meyer-Hofmeister & Meyer 1988). Results of a first rough investigation of the effect of evaporation were presented earlier (Meyer & Meyer-Hofmeister 1994). Now the evolution of the cool disk is computed in detail using the coronal structure and evaporation rate by Liu et al. (1995) and the physical relations deduced in Sect. 2.

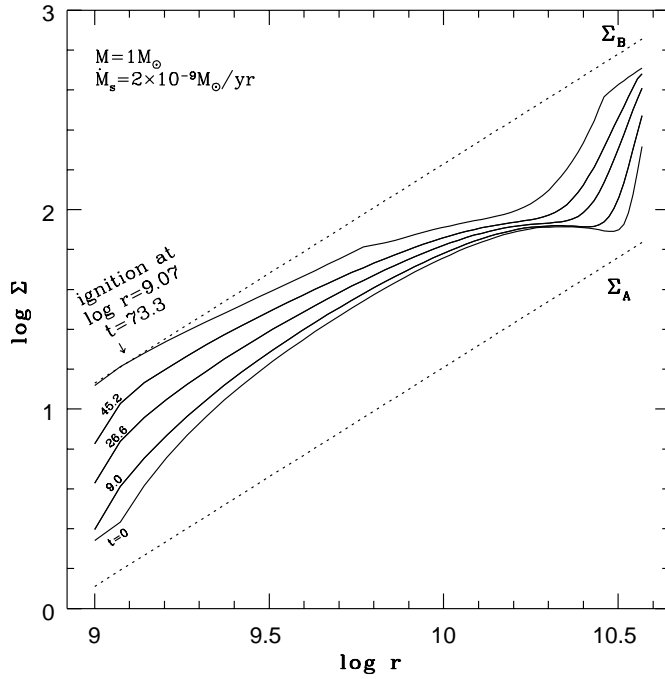


**Fig. 1.** Evolution of the disk during quiescence without evaporation.  $\Sigma$  surface density,  $r$  distance from central object. The two straight lines are critical surface densities. The diffusion time after outburst is indicated in days

#### 4.1. Computations including the relations derived in Sect. 2

During quiescence the matter flowing over from the secondary star is accumulated in the disk, only a small part is accreted onto the white dwarf. How the mass distribution changes depends on the assumed parameter  $\alpha$ . The smaller  $\alpha$  is the longer it takes for the gas to diffuse inward and the more matter is piled up in the outer disk. For outburst modelling the parameter  $\alpha$  is chosen to fit the duration of the quiescence. Both values,  $\alpha$  and the overflow rate (derived from observations), determine the evolving surface density distribution. A problem of dwarf nova outburst modelling was the fact that for adequately chosen  $\alpha$  and  $\dot{M}$  the onset of instability occurred dominantly in the innermost disk region (Cannizzo 1993, Ludwig et al. 1994, Ludwig & Meyer 1997), which is different from the observations.

For comparison we show in Fig. 1 the evolution of the disk without evaporation, in Fig. 2 including evaporation. Without evaporation the mass overflow from the secondary leads to a continuous increase of surface density everywhere in the disk. With evaporation the situation is different. From Fig. 2 one can see that the innermost disk is evaporated immediately after the preceding outburst. The inner boundary shifts outwards very fast at first and then more slowly. After 30 days a large hole is created and the inner boundary is at  $\log r = 9.63$ . At this distance from the white dwarf the evaporation has become very low and just about balances the low local quiescent mass flow there. This means that mass flow via the corona onto the white dwarf continues at a low rate. In connection with the mass accumula-

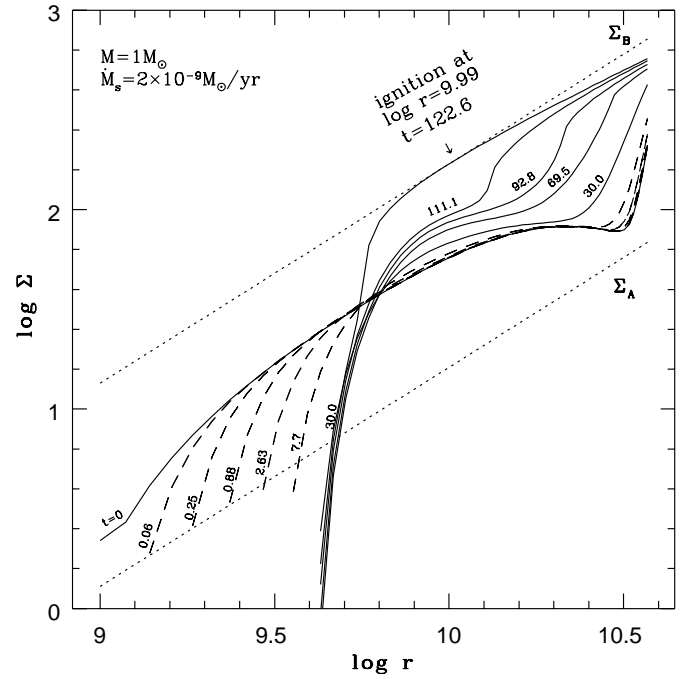


**Fig. 2.** Evolution of the disk during quiescence with evaporation. Parameters are same as in Fig. 1. Dashed lines show the preceding evaporation of the inner disk during early quiescence. For later quiescence the inner boundary stays at about the same distance from the white dwarf. The full lines show the evaporation after a large hole has been created until the next outburst is triggered

tion outside the hole the disk mass flow rate can increase and the boundary of the hole can then slightly be pushed inwards. Thus the observed X-rays and UV radiation in this later quiescence is expected to be low, maybe slightly varying. The consequence of the hole in the inner disk is accumulation of mass in the remaining outer disk. This leads to the onset of instability much farther out in the disk than without evaporation. Our new computations show that with the evaporation the onset of the outburst is at the distance of about  $10^{10}$  cm from the white dwarf, in much better agreement with the observations. The higher amount of matter needed to reach the critical surface density  $\Sigma_B$  at a larger radius demands a longer time of accumulation. In our example the onset of instability is found after 123 days with evaporation, after 73 days without evaporation. These are essential differences in the outburst behavior. Taking this into account one might then choose a larger value of  $\alpha$  for the quiescent state.

#### 4.2. Simplified computations

We compare our results with those of a simplified computation, where we take only the angular momentum away from the cool disk that is lost with the wind but neglect the angular momentum transport within the corona. The mass flow density  $\dot{m}_{d \rightarrow c}$  and the wind loss fraction  $\lambda$  are taken as derived by Liu et al. (1995),  $\dot{m}_{d \rightarrow c} = 10^{25.29} r^{-3.17} \text{ g cm}^{-2} \text{ sec}^{-1}$ ,  $\lambda = 0.25$ . The equations for conservation of mass and angular momentum in the cool

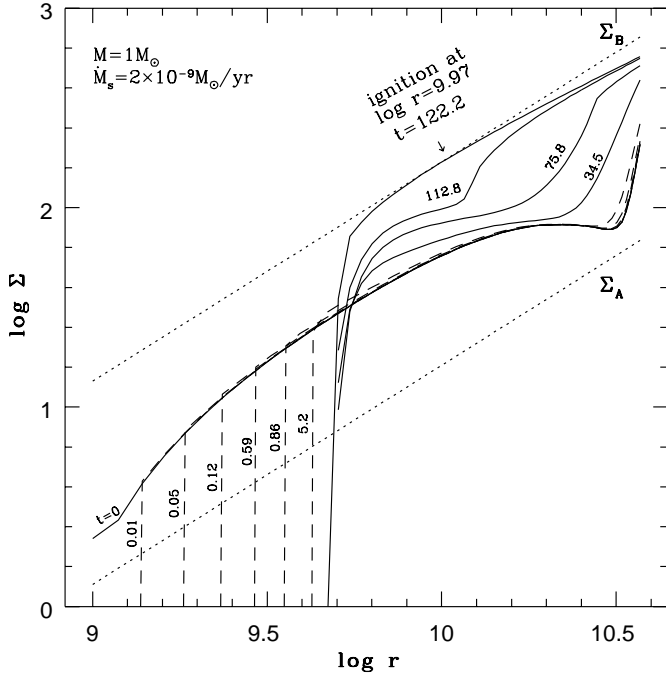


**Fig. 3.** Evolution of the disk during quiescence with evaporation in a simplified computation. Parameters are same as in Fig. 1. It shows similar evolution to Fig. 2 except for a very steep profile near the inner boundary

disk then are the same as Eqs. (3) and (4), except that at the right side of Eq. (4) the factor  $\lambda$  appears. Instead of relations (5) and (6) we have

$$\dot{M}_d = -3\pi(f_d + 2r \frac{\partial f_d}{\partial r}) + (1 - \lambda)4\pi r^2 \dot{m}_{d \rightarrow c} \quad (16)$$

$$\frac{\partial \Sigma_d}{\partial t} = \frac{3}{r} \frac{\partial}{\partial r} [r^{\frac{1}{2}} \frac{\partial}{\partial r} (r^{\frac{1}{2}} f_d)] + \dot{m}_{d \rightarrow c} [2 \times 3.17(1 - \lambda) - (5 - 4\lambda)] \quad (17)$$

This procedure conserves mass and angular momentum properly, it only restores the angular momentum released from coronal accretion locally to the disk.

The definition of the boundary is the same as the former (Sect. 3.3), i.e.  $f_d(r_i) = 0$ ,  $\dot{M}(r_i) = 0$ . From Eq. (16) follows  $(\frac{\partial f_d}{\partial r})_{r_i} = \frac{2}{3}(1 - \lambda)r_i \dot{m}_{d \rightarrow c}(r_i)$ , or

$$(\frac{\partial b}{\partial x})_{x_i} = \frac{1 - \lambda}{24} x_i^4 \dot{m}_{d \rightarrow c}(x_i) \quad (18)$$

We now obtain the location and the motion of the inner boundary under the influence of disk evolution and evaporation through  $b_{n_i} = b_i + (\frac{\partial b}{\partial x})_{x_i}(x_{n_i} - x_i)$  and Eq. (18) as

$$x_i = x_{n_i} - \frac{24}{1 - \lambda} \frac{b_{n_i}}{x_i^4 \dot{m}_{d \rightarrow c}(x_i)} \quad (19)$$

where  $x_{n_i}$  is the grid point closest to the inner boundary. This procedure does not require the solution of a transcendental equation (like Eq. (15)).

The results of this simplified calculation are shown in Fig. 3. One sees that the size of the hole, the duration of quiescence, the location where the critical surface density is reached are very similar to the former results. However, the profile of the surface density distribution near the inner boundary is much steeper than the former analytical “tail”, obviously it is caused by the rough approximation of the inner boundary motion, such a steep profile also occurs when interactions between disk and corona are taken into account but no analytical “tail” is included. In fact, the profile of the  $\Sigma$  distribution of the boundary just affects the time needed to create the hole during the early evolution, it hardly affects the final state before the outburst is triggered.

The fact that the two methods lead to so similar results illustrates that redistribution of angular momentum by the corona is not important. The changes of angular momentum only concern the region near the inner boundary and the amount of angular momentum there is small compared to that in the outer region.

## 5. Conclusions

Our computations show that mass flow via a vertically extended hot corona above the cool disk has three consequences as following.

### 5.1. UV-delay

A self-sustained corona disk can lead to an evaporation of the inner disk region. This is the part from which the UV is emitted during the outburst, the state of high mass flow in the disk. If a hole has been formed during quiescence it has first to be filled again in the next outburst before this radiation can appear. This needs a mass diffusion time and results in a lag of the rise in UV light compared to the optical which comes from more outer disk regions. This provides a natural explanation for the delay between optical and UV radiation at rise to outburst observed for some dwarf novae.

### 5.2. X-rays during quiescence

The evaporation rate changes with the size of the hole and thus does the accretion onto the white dwarf fed by this process. In the corona and at the white dwarf X-rays are produced, the major part coming from the white dwarf boundary layer (Liu et al. 1995). We expect a decreasing X-ray emission during the creation of the hole. Further changes depend on the situation in the cool disk, whether the inner disk boundary stays at a fixed location. These changes explain the variation of X-ray emission observed for many dwarf novae as we have shown in la Dous et al. (1997). We point out that the creation of a hole is an event in the early quiescence. Whether a hole is created at all depends on the mass distribution left over from the last outburst. ROSAT observations for the dwarf nova Z Cha taken weeks to months after the last outburst therefore can not show signatures of hole formation. Van Teeseling (1997) argued that a decreasing flux should be expected due to the evaporation model. But this is not the case so late after the outbursts. The observations are

in agreement with the theory for a phase of accretion via the corona at a moderate rate during late quiescence.

### 5.3. Onset of the outburst

The accumulation of the matter in the cool disk is changed. Without evaporation the recent computations for dwarf nova outbursts (Cannizzo 1993, Ludwig et al. 1994, Ludwig & Meyer. 1997) all show a tendency that the onset of instability occurs near the inner edge of the disk (which is close to the white dwarf in these investigations). In our computations, including evaporation, this is different, for the chosen parameters the onset of the outburst occurs at  $\log r = 9.99$ . The effective temperature is 6023 K where the disk starts to turn into the hot state. This onset of the instability away from the inner edge of the disk is in better agreement with the observation.

Evaporation of an inner accretion disk region might also be expected in other close binary systems where the disk is cool, as in black hole transient sources.

*Acknowledgements.* B.F. Liu acknowledges the support by the exchange program between the Max-Planck Society and the Chinese Academy of Sciences.

## References

- Cannizzo J. K., 1993, ApJ 419, 318  
la Dous C. 1994, Space Science Reviews 67, 1  
la Dous C., Meyer F., Meyer-Hofmeister E., 1997, A&A 321, 213  
King, A.R., 1997, MNRAS, in press  
Liu F.K., Meyer F, Meyer-Hofmeister E. 1995, A&A 300, 823  
Livio M., Pringle J. E., 1992, MNRAS 259, 23p  
Ludwig K., Meyer-Hofmeister E., Ritter H., 1994, A&A 290, 473  
Ludwig K., Meyer F., 1997, submitted to A&A  
Meyer F., 1997, in Accretion Disks – New Aspects, Lecture Notes in Physics, vol. 487, eds. E. Meyer-Hofmeister, H. Spruit, Springer-Verlag, p.338  
Meyer F., Meyer-Hofmeister E., 1989, A&A 221, 36  
Meyer F., Meyer-Hofmeister E., 1994, A&A 288, 175  
Meyer-Hofmeister E., Meyer F, 1988, A&A 194, 135  
van Teeseling, A., 1997, A&A 319, 125  
Verbunt F., 1987, A&AS 71, 339